DOI: 10.61782/fa.2025.0645

FORUM ACUSTICUM EURONOISE 2025

ON THE ACOUSTIC INVESTIGATION OF COMPLEX BUILDINGS MATERIALS BY PHYSICS INFORMED NEURAL NETWORKS (PINN)

Shahariar Ryehan[1*] **Ifat Zahan Soma**[2] **Juliette Naumann**[3]
[1] Department of Civil Engineering, University of Coimbra, Portugal
[2] Department of Mathematics, Hajee Mohammad Danesh Science and Technology University, Bangladesh
[3] Faculté des Sciences, Aix Marseille Université, France

ABSTRACT

Architects always use a range of aesthetic elements, including fractionally graded materials (FGMs), at a high acoustic and thermal demand level. Numerous partial differential equations, especially wave equations, have previously been the focus of extensive analytical or numerical approaches. However, the application of Neural Networks guided by physics raises the standard for acoustic results. Using the novel paradigm outlined in that paper, metal-ceramic composites, for instance, demonstrate extremely effective wave behavior to demonstrate changes in stiffness and density, including radiation, scattering, and noise transmission. Several kinds of PINN can help precisely define the error when comparing square error, absolute error, and mean square error compared to finite element simulations. The MATLAB NEURAL simulation for neural network toolboxes were used to view the simulation in this research. The research revealed that the results were extremely accurate, with a maximum inaccuracy of 2.6%. Intending to improve the acoustic management of homogenous materials, this study correspondingly examines the impact of material gradient on reflection and sound insulation properties. This suggested strategy offers a highly motivated basis for resolving wave propagation, opening the door to far better soundproofing outcomes, noise management, and more effective building material design.

[*]***Corresponding author***: *sryehan@gmail.com*

Keywords: *Physics Informed Neural Network (PINN), Fractional Graded Materials (FGMs), Acoustic Complex Buildings materials, Wave Propagation.*

1. INTRODUCTION

The development of new materials is greatly aided by recent developments in the field of materials science and engineering, which have made it possible for researchers to make judgments more quickly and accurately. Designing innovative materials requires the use of sophisticated mathematical models and appropriate neural network implementation. Artificial intelligence (AI) has become a necessity in many sectors, such as medicine [1], mechatronics [2], and aerodynamics [3], in the modern world. One of the famous Neural Network model - Physics-Informed Neural Networks (PINNs), which are successful in resolving challenging scientific and technical issues, is especially significant in this study. It is currently effectively used in a number of fields, including semiconductor technology [4], robotics [5], nuclear reactors [6], fatigue fracture analysis [7], blood flow monitoring [8], and lithium-ion batteries [9]. Its application is also noteworthy in domains including fluid dynamics modeling [10], safety control [11], and signal processing [12]. However, choosing the right material for a given application is one of the biggest hurdles in research. This study examines how well fractional gradient-descent-based composite materials work to address the issues of building thermal control and acoustic noise reduction. Zinc or aluminium oxide [13], Inconel-stainless steel [14], zirconium-aluminum [15], and natural materials like bamboo [16] can all be used to create these composite materials. The Navier-Stokes Equation, a renowned partial differential equation (PDE), is employed in this work to calculate the stress and elasticity of various materials, thereby assessing their suitability in building construction. Currently, the Finite Element Method (FEM) is used to get numerical solutions [17]; however, neural network-based solutions have received very little attention. Structure-Based PINNs [18], Variable Scaling PINNs [19], Fee PINNs [20], Runge-Kutta PINNs [21], and Flow Neural Networks [22] are among the prominent techniques for applying Physics-Informed Neural Networks (PINNs) to various structures. With these techniques, several modeling approaches can be enhanced through the use of the Loss-Weighted Algorithm or Loss Function Optimization [23], which can be applied to thermal modeling [24], hydrogen energy systems [25], and water hammer modeling [26]. The Helmholtz Equation [27], Fokker-Planck Equation [28], Time-Fractional Telegraph Equation [29], and Stochastic Differential Equation [30] are a few prominent examples of mathematical problems that can be directly solved using PINNs.

PINN's approach finds answers to the wave equation, which is comparable to actual waves, using epoxy-based training. This solution can be used to determine the frequency, refraction, reflection, wave speed, and ability to pass through the noise material. Even though the approach is still in the experimental stage and not as reliable as other numerical methods, it is continually being refined. Consequently, error analysis has been carried out in this study.

The equation that served as the foundation for the answer was identified in the first stage. The properties of the fractional gradient material were examined in the second step. The impact of multidimensional values was assessed in the third step, which involved a critical discussion of the wave function and its structure. Finally, by analyzing the findings and measuring the inaccuracies, potential avenues for further research have been suggested.

2. EQUATION MATHEMATICAL ANALYSIS

To investigate energy and other important properties for acoustic study of a material, one of the key aspects to consider is wave behavior. However, studying the wave function of a material often involves solving multiple partial differential equations. This study's analysis of the governing equation of the Navier-Stokes Elastic Motion Equation can provide new insights into the topic for an FGM material, if the displacement is U, the stress is δ and density is ρ then the elastic motion will be,

$$\delta_{xxx} + \delta_{yxy} + F_x = \rho U_{xtt} \qquad (1)$$
$$\delta_{yyy} + \delta_{xyx} + F_y = \rho U_{ytt} \qquad (2)$$

Where, $\delta_{xxx} = \frac{\partial^3 \delta}{\partial x^3}$.

Another way if we consider strain $\mathcal{E}$, we can get the comparison with wave function that,

$$\mathcal{E}_{xx} = U_{xx}, \qquad (3)$$
$$\mathcal{E}_{yy} = U_{yy}, \qquad (4)$$
$$\mathcal{E}_{xy} = \frac{U_{xy}+U_{yx}}{2} \qquad (5)$$

By using Hooke's law, we may get the following relations if we consider Young's Modulus as Ξ and Poisson's Ratio as ϱ,

$$\delta_{xx} = \frac{\Xi}{(1+\varrho)(1-2\varrho)}\left[(1-\varrho)\mathcal{E}_{xx} + \varrho\mathcal{E}_{yy}\right] \qquad (6)$$
$$\delta_{yy} = \frac{\Xi}{(1+\varrho)(1-2\varrho)}\left[(1-\varrho)\mathcal{E}_{yy} + \varrho\mathcal{E}_{xx}\right] \qquad (7)$$
$$\delta_{xy} = \frac{\Xi}{(1+\varrho)}\mathcal{E}_{xx} \qquad (8)$$

Placing the values of δ_{xx}, δ_{yy} and δ_{xy} in equations 1 and 2, we will get,

$$\frac{\Xi(1-\varrho)}{(1+\varrho)(1-2\varrho)}U_{xxx} + F_x = \rho U_{xtt} \qquad (9)$$
$$\frac{\Xi}{2(1+\varrho)}U_{yxx} + F_y = \rho U_{ytt} \qquad (10)$$

These two equations are the Navier-Stokes Elastic Motion Equations for the x and y axes, respectively.

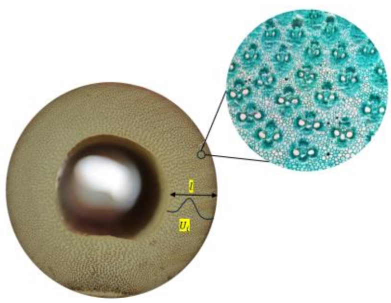

Figure 1. Cross section of FGM material, Bamboo as an example [31].

2.1. COORDINATES AND LOSS ANALYSIS

For wave function analysis, a layer-based (sliced) approach has been used in this study. Serial numbers i=1,2,3,...,n etc., have been assigned to each layer employed in the investigation, with L (m) representing each layer's thickness. For this stacking in the global coordinate system XOY, the necessary mathematical equations have been formulated. The fact that every layer is composed of the same kind of material and has been deemed to be flawless is notable. This approach has made it feasible to examine the waves' characteristics and motion in more depth. Then equation (9) would be,

$$\frac{\Xi_i(1-\varrho_i)}{(1+\varrho_i)(1-2\varrho_i)} U_{i_{xx}} + F_i = \rho_i U_{i_{tt}},\ i = 1,2,3,\dots,n \qquad (11)$$

For this we will get the loss function of the governing equation would be,

$$\mathcal{L}_{ge}(x,t) = \frac{1}{SR}\sum_{i}^{n}\sum_{r}^{R}\sum_{s}^{S}\left|\frac{\Xi_i(1-\varrho_i)}{(1+\varrho_i)(1-2\varrho_i)} U_{i_{xx}} + F_i - \rho_i U_{i_{tt}}\right|^2 \qquad (12)$$

Along the x-axis, the initial properties of the structure (displacement and particle velocity) determine the initial state, which is used as the starting conditions of the system.

$$U_i(x_i,t) = U_i(x_i,0) = G_i(x)\ ,\ i = 1,2,3,\dots,n \qquad (13)$$
$$U_{i_t}(x_i,t) = U_i(x_i,0) = F_i(x), i = 1,2,3,\dots,n \qquad (14)$$

Then the loss function using initial condition will be concerned as,

$$\mathcal{L}_{ic}(x,t) = \frac{1}{S}\sum_{i}^{n}\sum_{s}^{S}|U_i(x_{is},0) - G_i(x_{is})|^2 + |U_{is}(x_{is},0) - F_{is}(x_{is})|^2 \qquad (15)$$

This is the analogous boundary condition if the displacement stress is applied to the first layer surface for $x_1 = 0$. We will get,

$$U_1(x_1,t) = U_i(0,t) = Q(t_k) \qquad (16)$$
$$U_n(x_n,t) = U_n(H_n,t) = 0 \qquad (17)$$
$$U_n(x_n,t) = U_n(0,t) = 0 \qquad (18)$$

In this case, according to the hybrid-handed coordination method, the boundary conditions must be described separately for layers with odd and even serial numbers (n). According to the characteristics of n, the loss function and the form of the boundary condition will be different for even and odd numbers of boundaries

$if\ n = 2\kappa,$

$$\mathcal{L}_{bc}(x,t) = \frac{1}{R}\sum_{k}^{K}|U_1(0,t_k) - Q(t_k)|^2 + |U_n(H_n,t_k)|^2 \qquad (19)$$

$if\ n = 2\kappa \pm 1,$

$$\mathcal{L}_{bc}(x,t) = \frac{1}{R}\sum_{k}^{K}|U_1(0,t_k) - Q(t_k)|^2 + |U_n(0,t_k)|^2 \qquad (20)$$

When the structure consists of a single layer, the requirements above are sufficient to solve Navier's equations. If the layered structure has more than one layer, more consistency requirements are needed. The "consistency condition" refers to the requirement that the displacement and stress stay constant at every interface of the layered structure. The following is one way to express these conditions:

$$U_{2\alpha}(H_{2\alpha},t) = -U_{2\alpha-1}(H_{2\alpha-1},t) \qquad (21)$$
$$\delta_{2\alpha}(H_\alpha,t) = \delta_{2\alpha-1}(H_{2\alpha-1},t) \qquad (22)$$
$$U_{2\alpha}(0,t) = -U_{2\alpha+1}(0,t) \qquad (23)$$
$$\delta_{2\alpha}(0,t) = \delta_{2\alpha+1}(0,t) \qquad (24)$$

This also requires a loss function of compatibility, which will vary over even and odd.

$if\ n = 2\kappa$

$$\mathcal{L}_c(x,t) = \sum_{\alpha}^{n/2}\sum_{r}^{R}|U_{2\alpha}(H_{2\alpha},t_k) + U_{2\alpha-1}(H_{2\alpha-1},t_k)|^2 + |U_{2\alpha_x}(H_{2\alpha},t_k) - U_{2\alpha-1_x}(H_{2\alpha-1},t_k)|^2 + \sum_{\beta}^{n-2/2}\sum_{r}^{R}|U_{2\beta+1}(0,t_k) + U_{2\beta}(0,t_k)|^2 + |U_{2\beta+1_x}(0,t_k) - U_{2\beta}(0,t_k)|^2 \qquad (25)$$

$if\ n = 2\kappa \pm 1$

$$\mathcal{L}_{cc}(x,t) = \sum_{\alpha}^{n-1/2}\sum_{r}^{R}|U_{2\alpha}(H_{2\alpha},t_k) + U_{2\alpha-1}(H_{2\alpha-1},t_k)|^2 + |U_{2\alpha_x}(H_{2\alpha},t_k) - U_{2\alpha-1_x}(H_{2\alpha-1},t_k)|^2 + \sum_{\beta}^{n-1/2}\sum_{r}^{R}|U_{2\beta+1}(0,t_k) + U_{2\beta}(0,t_k)|^2 + |U_{2\beta+1_x}(0,t_k) - U_{2\beta}(0,t_k)|^2 \qquad (26)$$

The overall loss function of a system of multiple PINNs (Physics-Informed Neural Networks) is the sum of the loss functions of all sub-PINNs, which is composed of four main components:

$$\mathcal{L}_{total}(x,t) = \mathcal{L}_{ge} + \mathcal{L}_{ic} + \mathcal{L}_{bc} + \mathcal{L}_{cc} \qquad (27)$$

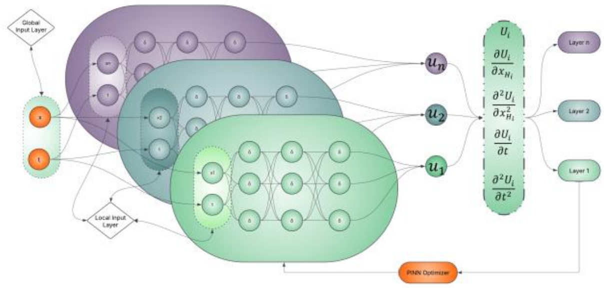

Figure 2. Diagrammatic illustration of the physics-informed neural network framework of the governing equations.

3. SOLUTION ANALYSIS

In physics, analytical methods for solving partial differential equations (PDEs) are often theoretically correct, but they have some limitations in practical applications. But in that research, to the extent possible, the result can overcome these limitations; we have considered two different boundary conditions in our study:

Table 1. Types according to their boundary condition

	Fixed-Fixed
Initial Boundary	$U(0,t)=0$ $U(H_1,t)=0$
Displacement	$U(x,0)=G(x)=0$
Velocity	$U_x(x,0)=F(x)=100000\times\pi\sin(3\pi x/H)$
Solutions	$U(x,t)=K_0 t+\sum_{f=0}^{f=n} K_f\cos\left(\frac{f\pi}{H}\right)\sin\left(\frac{f\pi c}{H}t\right)$ Where, $K_f=\frac{2}{f\pi c}\int_0^h G(x)\sin\left(\frac{f\pi x}{H}\right)dx$ And $K_0=\frac{1}{H}\int_0^H G(x)\,dx$
Bulk wave velocity	$c=\sqrt{\frac{\Xi(1-\varrho)}{(1+\varrho)(1-2\varrho)\rho}}$
	Free-Free
Initial Boundary	$U_x(0,t)=0$ $U_x(H_1,t)=0$
Displacement	$U(x,0)=G(x)=0$
Velocity	$U_x(x,0)=F(x)=100000\times\pi\sin(3\pi x/H)$
Solutions	$U(x,t)=\sum_{f=0}^{f=n} K_f\sin\left(\frac{f\pi}{H}\right)\sin\left(\frac{f\pi c}{H}t\right)$ Where, $K_f=\frac{2}{f\pi c}\int_0^H G(x)\sin\left(\frac{f\pi x}{H}\right)dx$
Bulk wave velocity	$c=\sqrt{\frac{\Xi(1-\varrho)}{(1+\varrho)(1-2\varrho)\rho}}$

In this article, "Gigantochla Scortechini (a species of bamboo found in Indonessia)" is used as an example of the Gradiant Descent metarials for the entire test [31]

Table 2. Materials Property

Properties	Values
Density	751 Kg/m^3
Poisson's ratio	0.27
Young's Modulus	20Gpa

4. RESULTS ANALYSIS:

The study's material has a density of 751 kg/m^3, a Poisson's ratio of 0.27, a Young's modulus of 20×10^9 Pa, and a thickness of 10 cm. These parameters indicate that the material displays the wave behavior depicted in Figure 3. As for the fixed-fixed situations, the time is stable, where the velocity function used in the analysis is F(x) and the global variable is one second. On the contrary, in free-free boundary conditions, the boundary changes over time, and the other space dimension coordinates, where x is divided into 100 equal parts. Here, a coefficient known as k_a is introduced, which, after ten iterative calculations, yields the optimal solution.

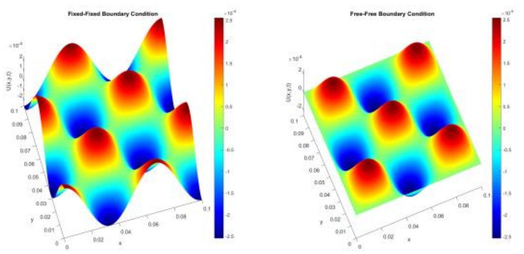

Figure 3. Analytical Wave Propagation Solution for Specified Material Parameters [32].

Finite element method (FEM) has been used in an advanced way to find the wave propagation analysis. In this method, it has been possible to examine the propagation of waves in both the x and y directions using a single finite element. In the case of Finite Element Analysis, we have applied a very fine-scale mesh system, where the size of each element has been set to only 0.0001 m.

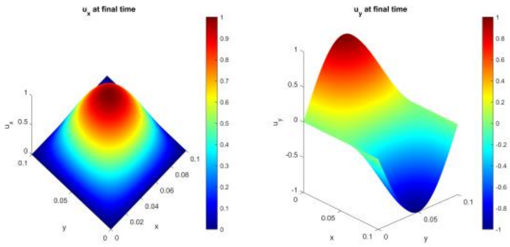

Figure 4. Numerical Wave Propagation Solution for both direction of x and y [32].

In this study, a deep neural network architecture to solve the wave equation. This network model, implemented on the matlab platform, consists of 4 fully connected hidden layers, each with 64 neurons, and includes a tanh function layer. We used 1,000 epochs in the training process of the model, which was sufficient to adequately train the network. Through this long-term training process, it will take almost 15 minutes, as shown in figure 6.

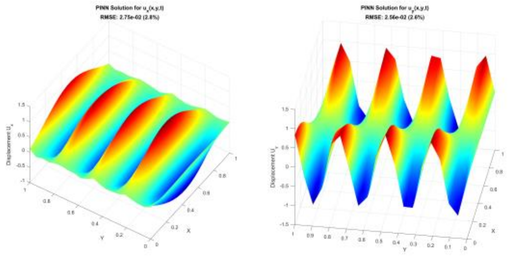

Figure 5. Wave Solution using physics-informed neural network [32].

5. PINN ERROR AND PERFORMANCE ANALYSIS

A clear relationship has been observed between the number of Epochs and the configuration of the hidden layer in the training process of the neural network model implemented in the study. The study has analysed 62000 iterations to optimize the training parameters, which used the MATLAB built-in function" trainingOptions", which progress visible on the training progress report.

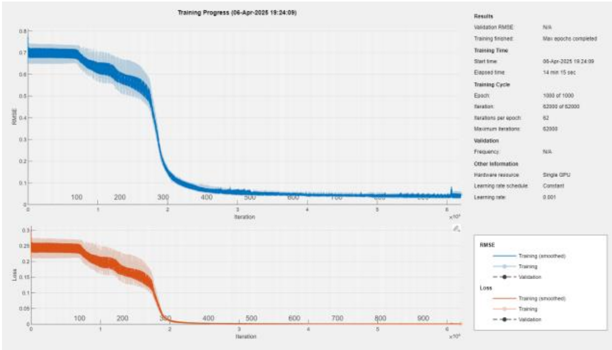

Figure 6. Training progress over time PINN [32].

Using Root mean square error (RMSE) figure 6 analyzed using the formula provided that,

$$RMSE = \sqrt{\frac{\sum_{i=1}^{n}(U_i - U_i')^2}{\sum_{i=1}^{n}(U_i')^2}} \tag{28}$$

Over a large number of iterations, it should approach nearly zero. Using equation (28), the error value is almost 2.6%, which is an excellent result. If this research were analyzed with more neurons and hidden layers, the result would be more accurate.

From the training progress, it's clearly visible that L_total (x,t), as given by equation (27), decreases over time. Furthermore, on maximum iteration, it's nearly zero. This means there is almost no loss in our wave result due to that training.

6. CONCLUSION

PINN (Physics-Informed Neural Network) has emerged as a breakthrough technology in acoustic technology research, which has revealed the experimental and numerical methods. The unique ability of this technology can occupied test using built-in parameters such as material thickness, density, Young's modulus etc., but can also accurately determine: Energy transfer rate through the material, Reflection and refraction coefficients, Theoretical properties of mechanical and physical properties
The study showed that the PINN method is able to provide results with an error of only 2.6% and loss nearly 0%, which has brought unprecedented accuracy to the material selection process. Features of this technology can be

improved by: Three-dimensional testing capability, Complex geometry easily analyse, because machine can breakthrough than FEM or analytical. This can provide effective ideal for multilayer materials like (functional gradient materials), can save convenient amount of time roughly 70% less computational time than conventional methods, High-dimensional problem-solving skills or Predictive power: Enables prediction of equipment performance, Provides guidelines for new material design, Nano-structured materials testing, Computer-assisted construction material development, Design optimization of sound-absorbing materials.

This has opened a new horizon in the construction industry, where the material selection process is now able to achieve unprecedented levels of knowledge technology precision and computational time. PINN-normal This method will play a significant role in the design and development of sustainable infrastructure to meet the goals of the coordination of principles.

7. ACKNOWLEDGMENTS

This work used MATLAB R2023a (Licensed) under an Institutional Student Agreement at Universitat Politècnica de València.

8. REFERENCES

[1] H. Mewada, I. M. Pires, M. Rahevar, and N. Khatri, “Quantum Convolutional Neural Network for Bone Fracture Classification from X-Ray Images,” Procedia Comput Sci, vol. 256, pp. 1143–1150, 2025.

[2] T. Taskov and J. Dushanova, “A simulated memristor architecture of neural networks of human memory,” Brain Organoid and Systems Neuroscience Journal, vol. 3, pp. 25–35, 2025.

[3] S. Baisthakur and B. Fitzgerald, “Physics-Informed Neural Network surrogate model for bypassing Blade Element Momentum theory in wind turbine aerodynamic load estimation,” Renew Energy, vol. 224, 2024.

[4] S. Ma, Y. Dang, Y. Sun, and Z. Yang, “A data-assisted physics-informed neural network for predicting fatigue life of electronic components under complex shock loads,” Int J Fatigue, vol. 197, p. 108933, 2025.

[5] T. Liquita Savio, R. Sanches Geronel, and M. M. da Silva, “Dynamic modeling of a novel catamaran robotic system actuated by bio-inspired propulsion devices using physics-informed neural networks,” Ocean Engineering, vol. 326, 2025.

[6] P. Baraldi, C. Battistini, F. Antonello, J. Buongiorno, and E. Zio, “Physics-Informed Neural Networks for the safety analysis of nuclear reactors,” Progress in Nuclear Energy, vol. 185, p. 105745, 2025.

[7] T. Huang, X. Li, Y. Zhang, L. Yao, and T. Zhang, “Multifactorial prediction of corrosion fatigue crack growth in aluminum alloys using physics-informed neural networks,” Eng Fail Anal, vol. 174, p. 109521, 2025.

[8] Y. Liu, L. Cai, Y. Chen, and Q. Chen, “ICPINN: Integral conservation physics-informed neural networks based on adaptive activation functions for 3D blood flow simulations,” Comput Phys Commun, vol. 311, 2025.

[9] C. Lin et al., “A lightweight two-stage physics-informed neural network for SOH estimation of lithium-ion batteries with different chemistries,” Journal of Energy Chemistry, vol. 105, pp. 261–279, 2025.

[10] S. Cai, Z. Mao, Z. Wang, M. Yin, and G. E. Karniadakis, “Physics-informed neural networks (PINNs) for fluid mechanics: a review,” 2021.

[11] X. Song, Y. Song, V. Stojanovic, and S. Song, “Improved Dynamic Event-Triggered Security Control for T–S Fuzzy LPV-PDE Systems via Pointwise Measurements and Point Control,” International Journal of Fuzzy Systems, vol. 25, no. 8, pp. 3177–3192, 2023.

[12] M. Sagib, B. K. Saha, S. K. Mohanty, and M. S. Rahman, “Diverse soliton solutions to the nonlinear partial differential equations related to electrical transmission line,” Phys Scr, vol. 99, no. 9, 2024.

[13] Hirshikesh, S. Natarajan, and E. T. Ooi, “Fatigue crack growth in functionally graded materials using an adaptive phase field method with cycle jump scheme,” Eng Fract Mech, vol. 312, 2024.

[14] A. A. Ferreira, A. R. Reis, J. P. Sousa, J. M. Cruz, and M. F. Vieira, “Inconel 625/NiCrWMo functionally graded materials manufactured by direct laser deposition,” Mater Charact, vol. 222, 2025.

[15] G. Gu, P. Wen, and F. Chen, “Rapid thermo-mechanical performance prediction and multi-objective optimization of tri-directional functionally graded material

considering complex geometry and arbitrary graded paths", 2025, Elsevier Ltd.

[16] S. Han, X. Hu, Y. Tao, S. Li, C. Xia, and G. Wang, "Construction relationship between a functionally graded structure of bamboo and its recombinant composite materials strength and toughness: Underlying mechanisms," Constr Build Mater, vol. 461, p. 139921, 2025.

[17] M. Wojciechowski, M. Lefik, and D. P. Boso, "Differential evolution algorithm and artificial neural network surrogate model for functionally graded material homogenization and design," Compos Struct, p. 119041, 2025.

[18] Z. Zheng, W. Jiang, Z. Wang, Z. Xiao, and Y. Guo, "Research on forward and inverse problems of structure based on physics-informed graph neural networks," Structures, vol. 74, p. 108618, 2025.

[19] S. Ko and S. Park, "VS-PINN: A fast and efficient training of physics-informed neural networks using variable-scaling methods for solving PDEs with stiff behavior," J Comput Phys, vol. 529, 2025.

[20] H. Zhang et al., "FE-PIRBN: Feature-enhanced physics-informed radial basis neural networks for solving high-frequency electromagnetic scattering problems," J Comput Phys, vol. 527, 2025.

[21] H. Li and C. Sun, "Nonlinear time-varying system response modeling via a real-time updated Runge-Kutta physics-informed neural network," Eng Appl Artif Intell, vol. 144, 2025.

[22] Z. Xiang, W. Peng, W. Yao, X. Liu, and X. Zhang, "Physics-informed Neural Implicit Flow neural network for parametric PDEs," Neural Networks, vol. 185, 2025.

[23] B. Gao, R. Yao, and Y. Li, "Physics-informed neural networks with adaptive loss weighting algorithm for solving partial differential equations," Computers and Mathematics with Applications, vol. 181, pp. 216–227, 2025.

[24] Y. Chen, H. Wang, and Z. Chen, "Sensitivity analysis of physical regularization in physics-informed neural networks (PINNs) of building thermal modeling," Build Environ, vol. 273, 2025.

[25] L. Zhang, J. Xie, Q. Xu, C. R. Koch, and S. Dubljevic, "Physics-informed neural networks for state reconstruction of hydrogen energy transportation systems," Comput Chem Eng, vol. 192, 2025.

[26] V. Tjuatja, A. Keramat, M. Rahmanshahi, and H.-F. Duan, "Spectral physics-informed neural network for transient pipe flow simulation," Water Res, vol. 279, p. 123427, 2025.

[27] C. Si and M. Yan, "Initialization-enhanced physics-informed neural network with domain decomposition (IDPINN)," J Comput Phys, vol. 530, 2025.

[28] Z. Jin, W. Zan, S. Ma, and W. Jia, "Physics-Informed Neural Networks with hybrid sampling for stationary Fokker–Planck–Kolmogorov Equation," Physica A: Statistical Mechanics and its Applications, vol. 663, 2025.

[29] F. Yang, H. Liu, X. X. Li, and J. X. Cao, "PINN neural network method for solving the forward and inverse problem of time-fractional telegraph equation," Results in Engineering, vol. 25, 2025.

[30] R. Gao, M. Yang, and J. Zhang, "Physics-informed generator-encoder adversarial networks with latent space matching for stochastic differential equations," J Comput Sci, vol. 79, 2024.

[31] N. A. Siam, M. Khairun, A. Uyup, H. Husain, A. L. Mohmod, and M. F. Awalludin, "Anatomical, Physical and Mechanical properties of Malesian Bamboo species," 2019.

[32] https://github.com/sryehan/pinn_FGM_sr